

Comparison of Data-driven Link Estimation Methods in Low-power Wireless Networks

Hongwei Zhang, *Member, IEEE*, Lifeng Sang, *Student Member, IEEE*, and Anish Arora, *Fellow, IEEE*

Abstract—Link estimation is a basic element of routing in low-power wireless networks, and data-driven link estimation using unicast MAC feedback has been shown to outperform broadcast-beacon based link estimation. Nonetheless, little is known about how different data-driven link estimation methods affect routing behaviors. To address this issue, we classify existing data-driven link estimation methods into two broad categories: *L-NT* that uses aggregate information about unicast and *L-ETX* that uses information about the individual unicast-physical transmissions. Through mathematical analysis and experimental measurement in a testbed of 98 XSM motes (an enhanced version of MICA2 motes), we examine the accuracy and stability of *L-NT* and *L-ETX* in estimating the ETX routing metric. We also experimentally study the routing performance of *L-NT* and *L-ETX*. We discover that these two representative, seemingly similar methods of data-driven link estimation differ significantly in routing behaviors: *L-ETX* is much more accurate and stable than *L-NT* in estimating the ETX metric, and, accordingly, *L-ETX* achieves a higher data delivery reliability and energy efficiency than *L-NT* (for instance, by 25.18% and a factor of 3.75 respectively in our testbed). These findings provide new insight into the subtle design issues in data-driven link estimation that significantly impact the reliability, stability, and efficiency of wireless routing, thus shedding light on how to design link estimation methods for mission-critical wireless networks which pose stringent requirements on reliability and predictability.

Index Terms—Low-power wireless networks, sensor networks, link estimation and routing, data-driven, beacon-based, distance-vector routing, geographic routing

I. INTRODUCTION

Wireless communication assumes complex spatial and temporal dynamics [1], [2], [3], [4], thus estimating link properties is a basic element of routing in wireless networks. One link estimation method that is commonly used in early wireless routing protocol design [5], [6] is letting neighbors exchange broadcast beacon packets, and then estimating link properties of unicast data transmissions via those of broadcast beacons. Nonetheless, unicast and broadcast differ in many ways such as transmission rate and MAC coordination method [7], [8], and it is difficult to precisely estimate unicast link properties via those of broadcast due to factors such as the impact that dynamic, unpredictable network traffic patterns have on link properties [9], [10].

The research community has become increasingly aware of the drawbacks of beacon-based link estimation, and has

proposed and started to use data-driven link estimation methods where unicast MAC feedback serves as the basis of link estimation [11], [12], [13], [14], [15], [6], [10]. In most wireless MAC protocols, a unicast packet is retransmitted, upon transmission failure, until the transmission succeeds or until the number of transmissions has reached a certain threshold value such as 8. For convenience, we call the individual transmissions involved in transmitting a unicast packet the *unicast-physical-transmissions*, and each unicast-physical-transmission represents a DATA-ACK handshake between the sender and the receiver. MAC feedback for a unicast transmission usually contains *aggregate* information (e.g., MAC latency, number of physical transmissions, and transmission status) about transmitting the unicast packet as a whole, but from these information we can derive properties of the *individual* physical transmissions involved in unicasting. Accordingly, we can classify existing data-driven link estimation methods depending on whether they use the aggregate information about unicast or they use information about the individual unicast-physical transmissions. As we will discuss in more detail in Section II-A, the existing data-driven link estimation methods can be represented by the following two seemingly similar methods of estimating link ETX (i.e., expected number of transmissions): *L-NT* where the aggregate information on the number of physical transmissions (NT) for each unicast is directly used to estimate link ETX, and *L-ETX* where the number of physical transmissions for each unicast is first used to calculate the reliability of individual unicast-physical-transmissions which is then used to estimate link ETX.¹

To clarify the subtle differences between *L-NT* and *L-ETX*, let us examine a simple example. Suppose we want to estimate the ETX metric along a link ℓ based on the MAC feedback $NTs = \{3, 4, 5\}$, which denotes the fact that it has taken 3, 4, and 5 physical transmissions to successfully deliver the first, second, and third unicast packet respectively. If it takes x number of physical transmissions to successfully deliver a unicast packet, then there are $(x - 1)$ number of failed physical transmissions and 1 successful physical transmission during this unicast. Accordingly, from NTs , we can derive a time series $TXes = \{0, 0, 1, 0, 0, 0, 1, 0, 0, 0, 0, 1\}$ denoting that the first and the second physical transmissions have failed, the third physical transmission has succeeded resulting the delivery of the first unicast packet, and the fourth physical transmission has failed, and so on. If we compute the packet delivery rate (PDR) of unicast-physical-

An extended abstract containing some preliminary results of this paper has appeared in IEEE SECON 2009.

Hongwei Zhang is with the Department of Computer Science, Wayne State University, Detroit, Michigan 48202, U.S.A. E-mail: hongwei@wayne.edu.

Lifeng Sang and Anish Arora are with the Department of Computer Science and Engineering, The Ohio State University, Columbus, OH 43210, U.S.A. E-mail: {sangl, anish}@cse.ohio-state.edu.

¹The letter “L” in the acronyms *L-NT* and *L-ETX* stands for “Learn on the fly”, which we used to denote the data-driven link estimation and routing protocol LOF [10].

transmissions based on the status (i.e., success or failure) of every 4 physical transmissions, then $TXes$ imply a time series $PDRs = \{0.25, 0.25, 0.25\}$ of the PDRs of unicast-physical-transmissions. Suppose we use the exponentially-weighted-moving-average (EWMA) estimator $\bar{x} = \frac{7}{8}\bar{x} + \frac{1}{8}x_k$. Then, in L-NT, the EWMA estimator is directly applied to $NTs = \{3, 4, 5\}$ to estimate ETX, and the estimated ETX value is 3.3594. In L-ETX, however, the EWMA estimator is first applied to $PDRs = \{0.25, 0.25, 0.25\}$ to estimate the average PDR, denoted by PDR_t , of unicast-physical-transmissions, then the link ETX is estimated to be $\frac{1}{PDR_t} = \frac{1}{0.25} = 4$.

As we will discuss in Section II-A, L-NT can represent the data-driven link estimation method used in SPEED [12], LOF [16], [10], and CARP [14] which employ aggregate MAC feedback information, and L-ETX can represent the data-driven link estimation method used in four-bit-estimation [11], EAR [13], NADV [15], and MintRoute[6] which employ the reliability information about individual unicast-physical-transmissions. Over the past years, various studies have shown that data-driven link estimation outperforms broadcast-beacon based link estimation in routing [10], [11], [14]. But little is known about how different data-driven link estimation methods affect routing behavior, and unicast MAC feedback has been used in mostly an ad-hoc manner. For instance, a L-NT-type and a L-ETX-type data-driven link estimation methods were first introduced in SPEED [12] and MintRoute[6] respectively; then two slightly different L-ETX-type estimation methods were used in NADV [15] and EAR [13], and a L-NT-type estimation method was used in LOF [16]; later, a L-ETX-type estimation method was used in four-bit-estimation [11], after which a L-NT-type estimation method was recently used again in CARP [14]. Some of the aforementioned protocols (e.g., SPEED [12] and four-bit-estimation [11]) are well known and well cited within the research community; some of these protocols have been deployed in field sensor networks, for instance, LOF [16] being deployed in the DARPA ExScal [17] project and four-bit-estimation [11] being adopted as the default link estimator in the TinyOS CTP protocol [18] and deployed accordingly. Nonetheless, we still lack a systematic understanding on how these different data-driven link estimation methods affect the reliability, latency, stability, and energy efficiency of routing. This is an important problem because, as low power wireless sensor networks are increasingly deployed for mission critical tasks such as industrial monitoring, it is critical to ensure high reliability, low latency, and high predictability in routing. Moreover, as the rich information carried in MAC feedback (e.g., both the number of physical transmissions and the time taken for a unicast transmission) are used in an increasingly broader context, it is important to understand the impact of the different ways of using these information.

Therefore, our objectives in this paper are to comparatively study the different methods of data-driven link estimation and to distill the guidelines of using MAC feedback information in wireless link estimation and routing. Through mathematical analysis and experimental measurement in a testbed of 98 XSM motes (an enhanced version of MICA2 motes), we examine the accuracy and stability of L-NT and L-ETX in

estimating the ETX routing metric. Using traffic traces for both bursty event detection and periodic data collection and using both grid and random network topologies, we also experimentally study the routing performance of L-NT and L-ETX. We discover that these two representative, seemingly similar methods of data-driven link estimation differ significantly in routing behaviors. L-ETX is much more accurate and stable than L-NT in estimating the ETX metric, and L-ETX correctly identifies the optimal routes with a higher probability than L-NT does. Accordingly, L-ETX achieves a higher data delivery reliability, higher energy efficiency, and higher throughput than L-NT (for instance, by 25.18%, a factor of 3.75, and a factor of 3.53 respectively in our testbed); L-ETX also uses longer yet more reliable links, thus introducing lower data delivery latency and latency jitter than L-NT. We also find that the higher stability in L-ETX enables a much higher stability in routing, thus improving the predictability of routing performance which is critical to mission-critical networked control. These findings provide new insight into the subtle design issues in data-driven link estimation that significantly impact the reliability, latency, and predictability of wireless routing, thus shedding light on the principles of using MAC feedback information in mission-critical wireless networks.

The rest of the paper is organized as follows. We compare different methods of using MAC feedback in Section II, and we present the impact of link estimation accuracy on routing behaviors in Section III. We discuss protocols similar to L-NT and L-ETX, and we present additional performance evaluation results in Section IV. Finally, we discuss related work in Section V and make concluding remarks in Section VI.

II. METHODS OF DATA-DRIVEN ESTIMATION

In this section, we first present in more detail the two representative methods (i.e., L-NT and L-ETX) of data-driven link estimation, then we comparatively study their estimation accuracy via mathematical and experimental analysis.

A. Different data-driven estimation methods

Based on the discussion in Section I, we can classify existing data-driven link estimation methods depending on whether they directly use the aggregate information about unicast or they use information about the individual unicast-physical-transmissions. In the literature, SPEED [12], LOF [10], and CARP [14] use the aggregate information MAC-latency, yet protocols such as four-bit-estimation [11], EAR [13], NADV [15], and MintRoute[6] use the reliability information about individual unicast-physical-transmissions. In this paper, we mainly focus on the following two data-driven link estimation methods:

- L-NT: directly use feedback information on the *number of physical transmissions* (NT) to estimate the expected number of physical transmissions (ETX) required to successfully deliver a packet across a link;
- L-ETX: first use feedback information to estimate the reliability, denoted as PDR, of individual unicast-physical-transmissions, then estimate ETX as $\frac{1}{PDR}$.

More specifically, given the same time series of MAC feedback information on unicast transmissions along a link, L-NT and L-ETX try to estimate ETX_t and PDR_t respectively, where ETX_t is the ETX for the link and PDR_t is the expected reliability of unicast-physical-transmissions along the link. In L-NT, the time series input $\{x_i : i = 1, 2, \dots\}$ to its estimator is $\{NT_i : i = 1, 2, \dots\}$, where NT_i is the number of physical transmissions taken to *successfully* deliver the i -th unicast packet;² in L-ETX, the time series input $\{x_i\}$ is $\{PDR_{i'} : i' = 1, 2, \dots\}$, where $PDR_{i'}$ is the packet delivery rate of the i' -th window of unicast-physical-transmissions with window size W (i.e., the average delivery rate of the $((i' - 1) \times W + 1)$ -th, $((i' - 1) \times W + 2)$ -th, \dots , and the $((i' - 1) \times W + W)$ -th unicast-physical-transmission).

The rationale for considering the two methods L-NT and L-ETX are as follows:

- ETX is a commonly used metric in wireless network routing;
- Since MAC latency is approximately proportional to NT given a certain degree of channel contention, the parameter NT is tightly related to MAC latency such that L-NT also represents protocols (e.g., SPEED [12] and LOF [16]) that directly use MAC latency in routing; (we will examine routing methods that use MAC latency in Section IV, and will show that they behave similar to L-NT.)
- L-NT and L-ETX estimate the same link property ETX, which enables fair, simple comparison between different data-driven estimation methods and helps elucidate the different behaviors across different data-driven link estimation methods.

Based on this research design, L-NT represents the method used in SPEED, LOF, and CARP, and L-ETX represents the method used in four-bit-estimation, EAR, NADV, and MintRoute.

In what follows, we first mathematically analyze the differences between L-NT and L-ETX to gain basic insight into the behaviors of different link estimation methods, then we experimentally measure the behaviors of L-NT and L-ETX to corroborate the analytical observations.

B. Analysis of L-NT and L-ETX

In low-power, resource constrained wireless sensor networks, most routing protocols use simple, light-weight estimators such as the exponentially-weighted-moving-average (EWMA) estimator and its variations. Therefore, our analysis in this section focuses on the accuracy of estimating ETX for a wireless link via the commonly-used EWMA estimator. But the analytical results also apply to variations of the basic

²Note that, for the i -th unicast packet, NT_i is calculated based on the MAC feedback on the number NT'_i of physical transmissions incurred for the i -th unicast and the status (i.e., success or failure) of the i -th unicast. If the status shows success, then $NT_i = NT'_i$; otherwise, the feedback simply shows that the packet has not been successfully delivered after transmitting NT'_i times, thus we set NT_i as $K \times NT'_i$, where K is a geometric random variable with success probability of P_i^u ($0 < P_i^u < 1$), and P_i^u is the average unicast reliability calculated based on the status information on transmitting the i unicast packets so far.

EWMA estimator such as the Window-Mean-with-EWMA (WMEWMA) estimator [6] and the Flip-Flop Filter (FF) [19].

Given a time series $\{x_i : i = 1, 2, \dots\}$ where x_i is a random variable with mean μ and variance σ^2 , the corresponding EWMA estimator for μ is

$$\begin{aligned} y_1 &= x_1 \\ y_k &= \alpha y_{k-1} + (1 - \alpha)x_k, \quad 0 \leq \alpha \leq 1, \quad k = 2, 3, \dots \end{aligned}$$

By induction, we have

$$y_k = \alpha^k x_1 + (1 - \alpha) \sum_{i=1}^k \alpha^{k-i} x_i, \quad k \geq 1$$

In what follows, we first analyze the accuracy of EWMA estimator in general, then we compare the accuracy of L-NT and L-ETX. For mathematical tractability, our analysis assumes that each unicast-physical-transmission is a Bernoulli trial with a failure probability P_0 ($0 \leq P_0 < 1$). We corroborate the validity of our analytical results through testbed-based experimental analysis in Sections II-C and III. We also discuss temporal link correlation at the end of this subsection.

Accuracy of EWMA estimators. To measure the estimation error in the estimator $\hat{\mu} = y_k$, we define *squared error* (SE) as

$$\begin{aligned} SE_k &= (y_k - \mu)^2 \\ &= ((\alpha^k x_1 + (1 - \alpha) \sum_{i=1}^k \alpha^{k-i} x_i) - \mu)^2 \\ &= (\alpha^k (x_1 - \mu) + (1 - \alpha) \sum_{i=1}^k \alpha^{k-i} (x_i - \mu))^2 \\ &= \alpha^{2k} (x_1 - \mu)^2 + (1 - \alpha)^2 \sum_{i=1}^k \alpha^{2(k-i)} (x_i - \mu)^2 + CP_k \end{aligned} \quad (1)$$

where

$$\begin{aligned} CP_k &= (1 - \alpha) \sum_{i=1}^k \alpha^{-i} (x_1 - \mu)(x_i - \mu) + \\ &= (1 - \alpha)^2 \sum_{i=1}^k \sum_{j \neq i, j=1}^k \alpha^{2k-i-j} (x_i - \mu)(x_j - \mu) \end{aligned}$$

Therefore, the *mean squared error* (MSE) is

$$\begin{aligned} MSE_k &= E[SE_k] \\ &= \alpha^{2k} E[(x_1 - \mu)^2] + \\ &= (1 - \alpha)^2 \sum_{i=1}^k \alpha^{2(k-i)} E[(x_i - \mu)^2] + \\ &= E[CP_k] \end{aligned} \quad (2)$$

Note that the expectation $E[\cdot]$ is taken over x_1, x_2, \dots, x_k .

When each unicast-physical-transmission is a Bernoulli trial, the x_i 's are mutually uncorrelated in both L-NT and L-ETX, that is, $E[x_i x_j] = E[x_i]E[x_j]$ if $i \neq j$,

$$\begin{aligned} E[(x_i - \mu)(x_j - \mu)] &= E[x_i x_j - x_i \mu - \mu x_j + \mu^2] \\ &= E[x_i]E[x_j] - \\ &= E[x_i]\mu - \mu E[x_j] + \mu^2 \\ &= 0 \end{aligned}$$

Thus,

$$\begin{aligned} E[CP_k] &= (1 - \alpha) \sum_{i=1}^k \alpha^{-i} E[(x_1 - \mu)(x_i - \mu)] + \\ &= (1 - \alpha)^2 \times \\ &= \sum_{i=1}^k \sum_{j \neq i, j=1}^k \alpha^{2k-i-j} E[(x_i - \mu)(x_j - \mu)] \\ &= 0 \end{aligned} \quad (3)$$

From Equations 2 and 3, we have

$$\begin{aligned} MSE_k &= \alpha^{2k} \sigma^2 + (1 - \alpha)^2 \sum_{i=1}^k \alpha^{2(k-i)} \sigma^2 \\ &= \sigma^2 \frac{2\alpha^{2k+1} - \alpha + 1}{1 + \alpha} \end{aligned} \quad (4)$$

To measure the *degree of estimation error* (DE) using estimator $\hat{\mu} = y_k$, we define DE_k as $\frac{\sqrt{MSE_k}}{\mu}$. Thus

$$\begin{aligned} DE_k &= \frac{\sqrt{MSE_k}}{\mu} \\ &= \frac{\sigma}{\mu} \sqrt{\frac{2\alpha^{2k+1} - \alpha + 1}{1 + \alpha}} \\ &= COV[X] \sqrt{\frac{2\alpha^{2k+1} - \alpha + 1}{1 + \alpha}} \end{aligned} \quad (5)$$

where $COV[X]$ is the coefficient-of-variation (COV) of the x 's, i.e., $COV[X] = \frac{\sigma}{\mu}$. Therefore, we have

Proposition 1: Assuming that x_i and x_j ($i \neq j$) are uncorrelated, the degree of estimation error using EWMA estimator is proportional to the COV of the x 's. \square

Relative accuracy of L-NT and L-ETX. To compare the DEs of L-NT and L-ETX, therefore, we first analyze the COV of NT_i and $PDR_{i'}$ as follows:

- L-NT: By definition, NT_i can be modeled as following a geometric distribution with the probability of success $1 - P_0$. Thus $E[NT_i] = \frac{1}{1 - P_0}$, and $std[NT_i] = \frac{\sqrt{1 - (1 - P_0)}}{1 - P_0} = \frac{\sqrt{P_0}}{1 - P_0}$. Therefore,

$$COV[NT_i] = \frac{std[NT_i]}{E[NT_i]} = \sqrt{P_0} \quad (6)$$

- L-ETX: Given a window size $W > 1$, the number N of successes in W physical transmissions can be modeled as following a Binomial distribution with the probability of success $1 - P_0$ and the number of trials W . Thus, $E[N] = W(1 - P_0)$, and $var[N] = W(1 - P_0)P_0$. Let $PDR_{i'} = \frac{N}{W}$, then $E[PDR_{i'}] = \frac{1}{W}E[N] = 1 - P_0$, $var[PDR_{i'}] = \frac{1}{W^2}var[N] = \frac{(1 - P_0)P_0}{W}$, and $std[PDR_{i'}] = \sqrt{var[PDR_{i'}]} = \frac{\sqrt{(1 - P_0)P_0}}{\sqrt{W}}$. Therefore,

$$COV[PDR_{i'}] = \frac{std[PDR_{i'}]}{E[PDR_{i'}]} = \frac{\sqrt{P_0}}{\sqrt{W(1 - P_0)}} \quad (7)$$

From Equations (6) and (7), we see that

$$COV[NT_i] > COV[PDR_{i'}], \text{ if } W > \frac{1}{1 - P_0} \quad (8)$$

Note that the condition $W > \frac{1}{1 - P_0}$ generally holds in practical scenarios, since W is generally greater than 2 and P_0 is generally less than 50% [20], [10].

From Proposition 1 and Inequality (8), then we have

Proposition 2: Given an EWMA estimator and assuming that each unicast-physical-transmission is a Bernoulli trial, $DE_k(\text{L-ETX}) < DE_k(\text{L-NT})$ if $W > \frac{1}{1 - P_0}$; that is, L-ETX is more accurate than L-NT in estimating the ETX value of a link as long as $W > \frac{1}{1 - P_0}$. \square

Proof sketch: We first show that $DE(\text{L-ETX}) \approx DE(\text{PDR})$ as follows. Let P_t be the actual $E[\text{PDR}]$, ETX_t be the actual ETX and equal to $\frac{1}{P_t}$, and P_e be the estimated $E[\text{PDR}]$. Then the absolute estimation error ΔETX of ETX is as follows:

$$\Delta ETX = \left| \frac{1}{P_e} - \frac{1}{P_t} \right| = \frac{1}{P_t} \left| \frac{P_t - P_e}{P_e} \right| = ETX_t \frac{|P_t - P_e|}{P_e}$$

Thus

$$DE(\text{L-ETX}) = \frac{E[\Delta ETX]}{ETX_t} = E\left[\frac{|P_t - P_e|}{P_e}\right] \approx DE[\text{PDR}].$$

In the mean time, we know from Proposition 1 and Inequality 8 that $DE_k(\text{L-NT}) > DE_k[\text{PDR}]$. Therefore, $DE_k(\text{L-NT}) > DE_k(\text{L-ETX})$. \square

From the above analysis, we see that, even though L-NT and L-ETX use the same MAC feedback information in a seemingly similar fashion (e.g., $\text{PDR}_{i'}$'s assume, approximately, a form of the reciprocal of NT_i 's), the variability (more precisely, the COV) of NT_i 's tends to be greater than that of $\text{PDR}_{i'}$'s, and this difference in variability makes L-NT a less accurate estimator than L-ETX.

Remarks on temporal link correlation. By assuming that each unicast-physical-transmission is a Bernoulli trial, the above analysis does not consider temporal link correlation. In general, temporal link correlation may affect analytical results on the accuracy of EWMA estimator and the COVs of NT_i and $\text{PDR}_{i'}$. For the purpose of this paper, however, temporal link correlation is less of a concern due to the following reasons:

- Even though the status (i.e., success or failure) of individual consecutive unicast-physical-transmissions tend to be correlated, the x_i 's in L-NT and L-ETX are much less correlated. This is because 1) the x_i 's in L-NT and L-ETX characterize the properties of unicasts which, spanning the time duration of several unicast-physical-transmissions, are well separated in time when compared with consecutive unicast-physical-transmissions, and 2) temporal link correlation tends to be high only for samples from a close, short time frame [20]. Therefore, even though the analysis on the accuracy of EWMA estimator assumes that x_i 's are uncorrelated in L-NT and L-ETX, the insights gained from the analysis do hold in practice as we will show in Sections II-C and III.
- For the purpose of analyzing expected transmission cost along wireless links, Keshavarzian *et al.* [21] showed that the *Block-Markov Model* captures the impact of block fading and is effective in characterizing temporal link correlation. In Block-Markov model, temporal link properties are captured with a random process $\{P_i, i \geq 1\}$, where P_i is the probability that the i -th packet transmission is successful. The P_i 's can possibly exhibit correlation, but, conditional on the values of the P_i 's, packet success events are independent of one another. For the random process $\{P_i, i \geq 1\}$, there exist an integer M , which reflects channel coherence time, and a random variable P ($0 \leq P \leq 1$) such that 1) $P_1, P_{M+1}, P_{2M+1}, \dots$ form an independent sequence with the same distribution as P , and 2) $P_1 = P_2 = \dots = P_M, P_{M+1} = P_{M+2} = \dots = P_{2M}, P_{2M+1} = P_{2M+2} = \dots = P_{3M}$, and so on. From the Block-Markov model, we see that the success probability of consecutive transmissions tends to be similar within a short timeframe (e.g., the timeframe of the channel coherence time which is usually at the scale of 500ms for static wireless networks [21], [22]).

Since packet success events can also be regarded as independent conditional on the P_i 's, the use of Bernoulli trials to model unicast-physical-transmissions tends to be a good approximation as far as computing expected link transmission cost is concerned.

We corroborate these analytical observations through experimental analysis in Sections II-C and III.

Remarks on the impact of W and α . Note that, even though they do not affect the relative accuracy of L-NT and L-ETX, the window size W used in L-ETX and the weight factor α of the EWMA estimator also affect estimation accuracy. In what follows, we briefly discuss the impact of W and α .

From Equations 5 and 7, we see that larger window size W will lead to smaller estimation error in L-ETX; on the other hand, a larger W leads to reduced agility for the estimator to respond to changes, which can negatively affect routing performance in the presence of network dynamics. In practice, we usually choose a medium-sized W as a tradeoff between estimation accuracy and agility, and W is set as 20 for the study of this paper.

Let $Q_k(\alpha) = \sqrt{\frac{2\alpha^{2k+1}-\alpha+1}{1+\alpha}}$, then, by Equation 5, DE_k is proportional to $Q_k(\alpha)$. Figure 1 shows the impact of α on

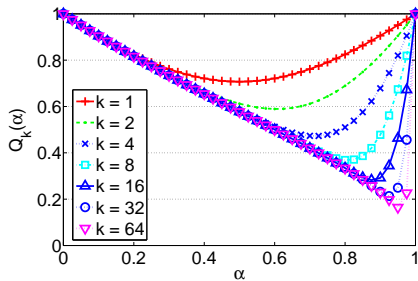


Fig. 1. $Q_k(\alpha)$

$Q_k(\alpha)$ and thus DE_k . We see that the optimal α value increases as k increases, and the intuition is that, as k increases, the contribution of the history data (i.e., x_0, x_1, \dots, x_{k-1}) to y_k becomes more and more important compared with that of the most recent observation x_k . On the other hand, the agility of the estimator decreases as α increases. After α exceeds certain threshold value, moreover, $Q_k(\alpha)$ (and thus DE_k) increases as α increases further. In practice, therefore, we can choose a value that tradeoffs between estimation precision and agility, and we set α as $\frac{7}{8}$ in our study.

C. Experimentation with L-NT and L-ETX

Having shown that L-ETX is a more accurate estimation method than L-NT in Proposition 2, we experimentally evaluate the validity of the analytical results and study the impact of estimation accuracy on the optimality and stability of routing using the *Kansei* [23] sensor network testbed. In what follows, we first present the experiment design and then the experimental results.

Experiment design. In an open warehouse with flat aluminum walls (see Figure 2(a)), *Kansei* deploys 98 XSM motes

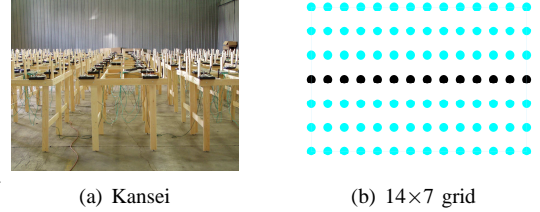


Fig. 2. Sensor network testbed *Kansei*

[24] in a 14×7 grid (see Figure 2(b)) where the separation between neighboring grid points is 0.91 meter (i.e., 3 feet). The grid deployment pattern enables experimentation with regular, grid topologies, as well as random topologies (e.g., by randomly selecting nodes of the grid to participate in experiments). XSM is an enhanced version of Mica2 [25] mote, and each XSM is equipped with a Chipcon CC1000 [26] radio operating at 433 MHz. To form multihop networks, the transmission power of the CC1000 radios is set at -14dBm (i.e., power level 3) for the experiments of this paper unless otherwise stated. XSM uses TinyOS [27] as its operating system. For all the experiments in this paper, the default TinyOS MAC protocol B-MAC [28] is used; a unicast packet is retransmitted, upon transmission failure, at the MAC layer (more specifically, the TinyOS component QueuedSend) for up to 7 times until the transmission succeeds or until the 8 transmissions have all failed; a broadcast packet is transmitted only once at the MAC layer (without retransmission even if the transmission has failed).

To collect measurement data on unicast link properties, we let the mote on the left end of the middle row (shown as black dots in Figure 2(b)) be the *sender* and the rest 13 motes of the middle row as the *receivers*, and we measure the unicast properties of the links between the sender and individual receivers. (Note that we have observed similar phenomena as what we will present in this section for other sender-receiver pairs.) The sender transmits 15,000 unicast packets to each of the receivers with a 128-millisecond inter-packet interval, and each packet has a data payload of 30 bytes. Based on packet reception status (i.e., success or failure) at the receivers, we measure unicast link properties.

To examine the impact of traffic-induced interference on link properties and link estimation, we randomly select 42 motes out of the light-colored (of color cyan) 6 rows as *interferers*, with 7 interferers from each row on average. Each interferer transmits unicast packets (of payload length 30 bytes) to a destination randomly selected out of the other 41 interferers. The load of the interfering traffic is controlled by letting interferers transmit packets with a certain probability d whenever the channel becomes clear. Ng *et al.* [29] showed that the optimal traffic injection rate is 0.245 in a regular linear topology, and the optimal traffic injection rate will be even lower in general, two-dimensional network. Thus our measurement study focuses more on smaller d 's than on larger ones, but we still study larger d 's to get a sense on how systems behave in extreme conditions. More specifically, we use the following d 's in our study: 0, 0.01, 0.04, 0.07, 0.1, 0.4, 0.7,

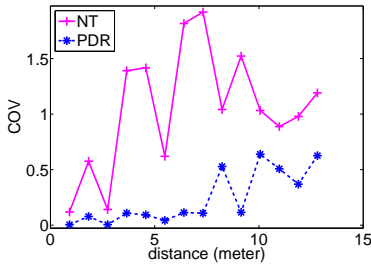


Fig. 3. COV[NT] vs. COV[PDR] when $d = 0.1$; Note that the reason why the COVs are not monotonic with link length (i.e., sender-receiver distance) is because of radio and environment variations [4]. In this paper, we use distance mainly to identify individual links associated with a sender, and for clarity of presentation, we do not present confidence intervals unless they are necessary for certain claims of the paper.

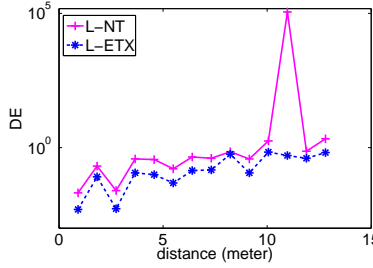


Fig. 4. DE(L-NT) vs. DE(L-ETX) when $d = 0.1$

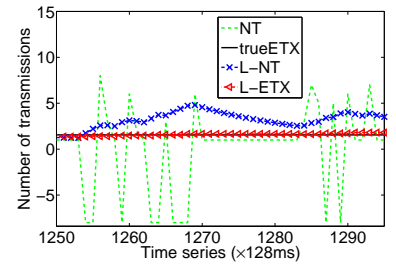


Fig. 5. Time series of estimated ETX values in L-NT and L-ETX for a link of length 9.15 meters (i.e., 30 feet); note that the time unit for the X-axis is 128 milliseconds.

and 1. Thus the interference pattern is controlled by d in this case. (Note that phenomena similar to what we will present have been observed for other interfering traffic patterns, for instance, with different spatial distribution and different number of interferers.) We have done the experimental analysis for different d 's and observed similar phenomena. Due to the limitation of space, here we only present data for the cases when $d = 0.1$ and $d = 0.7$. We first discuss the results for $d = 0.1$, then we discuss the results for $d = 0.7$.

Estimation accuracy. Figure 3 shows the COV of NT and PDR for different links. We see that COV[NT] is significantly greater, up to a factor of 17.78, than COV[PDR], which is consistent with our analysis as shown by Inequality 8. Accordingly, the degree of estimation error (DE) in L-NT is consistently greater than that in L-ETX, as shown in Figure 4 where DE(L-NT) and DE(L-ETX) for different links are presented. Therefore, the experimental results corroborate the prediction of Proposition 2. Note that the reason why, given an estimation method, the trend for its curves of COV and DE are slightly different (unlike what Equation 5 would suggest to be exactly the same) is due to the simplified assumption (i.e., each unicast-physical-transmission is a Bernoulli trial) used in the analysis. Nonetheless, the analytical and experimental analysis do agree on the relative accuracy between L-NT and L-ETX. The reason why the DE value for the 11-meter-long link is very large in L-NT is due to the extremely low reliability of the link and the fact, as we show immediately below, that L-NT introduces large estimation errors in the presence of transmission failures.

To elaborate on the details of link estimation, Figure 5 shows, for a link of length 9.15 meters (i.e., 30 feet), the time series of the estimated ETX values via L-NT and L-ETX respectively. (Note: the figure is more readable in color-print than black-white print.) To visualize the accuracy of L-NT and L-ETX, we also show the NT values carried in MAC feedbacks and the actual ETX value for the link. To easily represent a unicast transmission failure (after 7 retransmissions), we present -8 as the NT value for the corresponding unicast transmission. We see that the estimated ETX in L-NT tends to

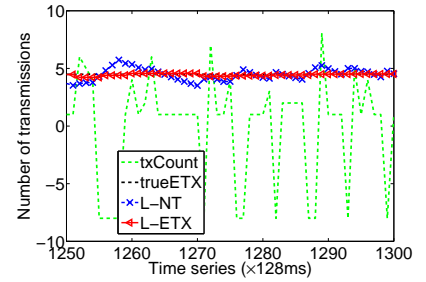
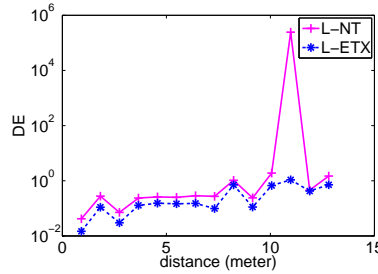
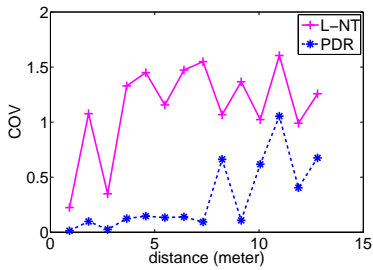
deviate from the actual ETX value, especially in the presence of MAC transmission failures; the estimated ETX in L-ETX, however, is very close to the actual ETX value, even in the presence of MAC transmission failures. We also see that the estimated ETX value in L-ETX is pretty stable whereas the estimation of L-NT oscillates significantly, which has significant implications to routing behaviors as we discuss next and in Section III-B. The reason why L-ETX performs so well in this case is because of the small coefficient-of-variation (COV) of the PDR and thus small estimation error.

Routing optimality and stability. To understand the routing behaviors in L-NT and L-ETX, we consider the case where the sender on the left end of the middle row of Figure 2(b) needs to select the best next-hop forwarder among the set of receivers in the middle row, and the destination is far away from the sender but in the direction extending from the sender along the middle row to the right. For simplicity, we assume that the sender uses a localized, geographic routing metric ETD (for *ETX per unit-distance to destination*) in evaluating the goodness of forwarder candidates. The metric ETD is defined as follows: given a sender S , a neighbor R of S , and the destination D , the ETD via R is defined as

$$\begin{cases} \frac{ETX_{S,R}}{L_{S,D} - L_{R,D}} & \text{if } L_{S,D} > L_{R,D} \\ \infty & \text{otherwise} \end{cases} \quad (9)$$

where $ETX_{S,R}$ is the ETX of the link from S to R , $L_{S,D}$ denotes the distance from S to D , and $L_{R,D}$ denotes the distance from R to D . We will show in Section IV that this local, geographic metric performs in a similar way as the global, distance-vector metric for uniform networks.

In our case, the best forwarder is 10 grid-hops away from the sender since the corresponding link has the minimum ETD value. To see how L-NT and L-EXT perform in selecting the next-hop forwarder, Table I shows the forwarders (identified in terms of their grid hop distance from the sender) used in L-NT and L-ETX respectively. To illustrate the optimality of different methods, we measure the percentage of time each forwarder is used, and the cost ratio of this forwarder to the optimal forwarder 10. We see that L-ETX is able to identify

Fig. 6. COV[NT] vs. COV[PDR] when $d = 0.7$ Fig. 7. DE(L-NT) vs. DE(L-ETX) when $d = 0.7$ Fig. 8. Time series of estimated ETX values when $d = 0.7$

| Method | Forwarder | Percentage (%) | Cost ratio |
|--------|-----------|----------------|------------|
| L-NT | 5 | 0.1 | 2.3 |
| | 6 | 4.14 | 1.3 |
| | 7 | 7.17 | 1.5 |
| | 8 | 21.26 | 1.3 |
| | 10 | 67.33 | 1 |
| L-ETX | 6 | 5.91 | 1.3 |
| | 7 | 0.2 | 1.5 |
| | 8 | 5.1 | 1.3 |
| | 10 | 88.79 | 1 |

TABLE I
FORWARDERS USED IN L-NT AND L-ETX WHEN $d = 0.1$

| Method | Forwarder | Percentage (%) | Cost ratio |
|--------|-----------|----------------|------------|
| L-NT | 3 | 33.74 | 1 |
| | 6 | 31.41 | 1.1 |
| | 7 | 1.92 | 1.7 |
| | 8 | 17.88 | 1.2 |
| | 10 | 15.05 | 1.2 |
| L-ETX | 3 | 70 | 1 |
| | 6 | 30 | 1.1 |

TABLE II
FORWARDERS USED IN L-NT AND L-ETX WHEN $d = 0.7$

and use the optimal forwarder more than 20% of the time compared with L-NT. The average ETD of using L-ETX is 3.26% more than the optimal ETD, yet the average ETD of using L-NT is 11.34% more than the optimal ETD.

We also measure the number of times that the sender changes its forwarder when using L-NT and L-ETX respectively, and we observe that the number of forwarder changes is 95 and 13 in L-NT and L-ETX respectively. Thus, L-ETX ensures much higher routing stability than L-NT, which is due to the fact that L-ETX is a more stable estimator than L-NT as can be seen from Figure 5. Higher routing stability helps improve the predictability of packet delivery performance in networks.

The case of $d = 0.7$. According to Ng *et al.* [29], the per-node traffic injection rate in a well-controlled multi-hop wireless network is usually less than 0.245. But to understand how L-NT and L-ETX behave in extreme conditions of heavy traffic load, here we briefly discuss the case of $d = 0.7$. Figures 6, 7, and 8 show the estimation accuracy of L-NT and L-ETX when $d = 0.7$, and Table II shows the routing optimality of L-NT and L-ETX when $d = 0.7$. We see that, compared with the case of $d = 0.1$, the ETX values of individual links are larger, and the COVs of L-NT and L-ETX are also slightly larger. This is due to the increased channel contention and co-channel interference as the interfering traffic load increases. Accordingly, the best forwarder becomes forwarder 3. Despite these changes, L-ETX still performs better than L-NT, introducing lower estimation errors and being able to identify the actual best forwarder with much higher probability.

III. ROUTING PERFORMANCE

Having discussed the significant impact that link estimation methods have on estimation accuracy and routing optimality in Section II, we experimentally evaluate the performance of different data-driven link estimation methods in this section. We first present the methodology and then compare different data-driven estimation methods.

A. Methodology

We use a publicly available event traffic trace for a field sensor network deployment [30] to evaluate the performance of different protocols. The traffic trace corresponds to the packets generated in the 7×7 grid of a field MICA2 mote network when a vehicle passes across the middle of the network. When the vehicle passes by, each mote except for the base station detects the vehicle and generates two packets, which correspond to the start and the end of the event detection respectively and are separated 5-6 seconds on average. Overall, 96 packets are generated each time the vehicle passes by. The cumulative distribution of the number of packets generated during the event is shown in Figure 9. (Interested readers can find the detailed description of the traffic trace in [30].) Since the traffic trace is collected from 49 nodes that are deployed in a 7×7 grid, we randomly select and use a 7×7 subgrid of the Kansei testbed (as shown in Figure 2(b)) in our experiments. To form a multi-hop network, we set the radio transmission power at -14dBm (i.e., power level 3). The mote at one corner of the subgrid serves as the base station, the other 48 motes generate data packets according to the aforementioned event traffic trace, and the destination of all the data packets is the base station. We also evaluate protocols with other traffic patterns, e.g., periodic data traffic, and other network setups,

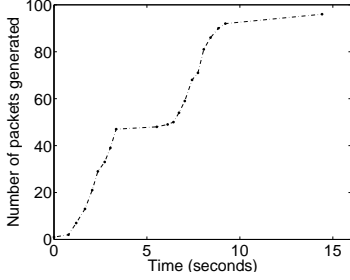


Fig. 9. The distribution of packets generated in the event traffic trace

e.g., random networks. We observe phenomena similar to what we will present, but we relegate the detailed discussion to Section IV.

Using the above setup, we comparatively study the performance of the following data-driven link estimation and routing protocols:³

- *L-NT*: a distance-vector routing protocol whose objective is to minimize the expected number of transmissions (ETX) from each source node to its destination. The ETX metric of each link (and thus each route) is estimated via the L-NT data-driven method.
- *L-ETX*: same as L-NT except that the ETX metric is estimated via the L-ETX method.
- *L-WNT*: a variant of L-NT where the input to the EWMA estimator is the average of 5 *NT* values for every 5 consecutive unicast transmissions. We study this protocol to check whether the performance of protocol L-NT can be improved by increasing the stability of the L-NT method through the window-based NT average.
- *L-NADV*: a variant of L-ETX where the window size W is 1 and the EWMA estimator is used to estimate packet error rate (PER) instead of PDR. We study this protocol mainly to examine the impact of W .⁴ L-NADV is also the distance-vector version of the geographic protocol NADV [15].

In the above data-driven protocols, periodic, broadcast beacons are never used. We use the approach of *initial link sampling* [10] to jump-start the routing process, where a node proactively takes 7 samples of MAC feedback (by transmitting 7 unicast packets) for each of its candidate forwarders and then chooses the best forwarder based on the initial sampling results.

For each protocol we study, we ran the event traffic trace sequentially for 40 times, and we measure the following protocol performance metrics:

- *Event reliability (ER)*: the number of unique packets received at the base station divided by the total number of unique packets generated for an event. This metric reflects the amount of useful information that can be delivered for an event.

³In this paper, we sometimes use the same name for the protocol, the estimation method, and the routing metric. The context of its usage will clarify its exact meaning.

⁴Our experiments show that routing performance is statistically the same whether we use PER or PDR as the input to the EWMA estimator.

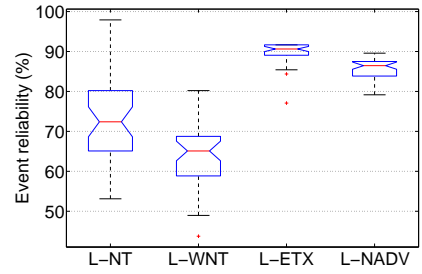


Fig. 10. Event reliability

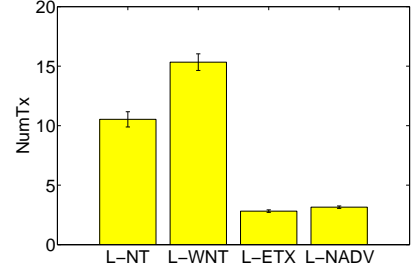


Fig. 11. Average number of transmissions per packet delivered, with the error bar representing the confidence intervals at the 95% confidence level

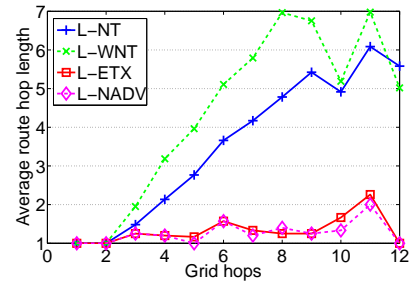


Fig. 12. Average route hop length for nodes different grid-hops away from the base station

- *Number of transmissions per packet delivered (NumTx)*: the total number of physical transmissions incurred in delivering packets of an event divided by the number of unique packets received at the base station. This metric affects network throughput; it also reflects the energy efficiency of a protocol, since it not only affects the energy spent in transmission but also the degree of duty cycling which in turn affects the energy spent at the receiver side.

We also compare data delivery latency and predictability using our data on the reliability and detailed properties of the routes used in different protocols.

B. Experimental results

Figures 10 and 11 show the event reliability and the average number of transmissions required for delivering each packet in different data-driven protocols respectively, Figures 12 and 13 show the average route hop length and

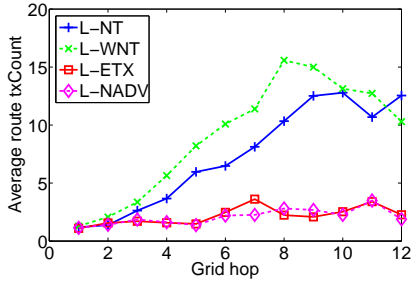


Fig. 13. Average route transmission count for nodes different grid-hops away from the base station

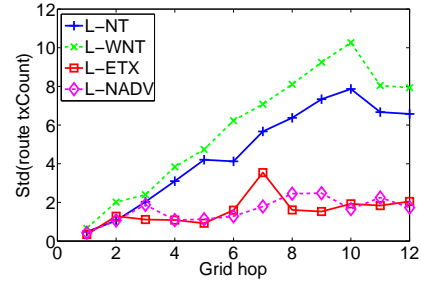


Fig. 14. Standard deviation of the route transmission count for nodes different grid-hops away from the base station

| Metric | L-NT | L-WNT | L-ETX | L-NADV |
|---|--------|--------|--------|--------|
| Average per-hop geo-distance (meter) | 2.89 | 2.51 | 4.17 | 4.37 |
| Average per-hop physical tx reliability | 56.3% | 51.08% | 68.43% | 66.77% |
| Average per-hop unicast reliability | 87.62% | 87.02% | 93.10% | 89.21% |
| Per-hop ETX | 2.56 | 2.65 | 1.94 | 2.18 |

TABLE III
PER-HOP PROPERTIES IN DIFFERENT ROUTING PROTOCOLS

route transmission count respectively for successfully delivered packets coming from nodes at different grid-hops away from the base station, and Table III shows the detailed information about the properties of the links used in different protocols.

L-NT vs. L-ETX. From Figure 10, we see that L-ETX achieves a significantly higher event reliability than L-NT. For instance, the median event reliability in L-ETX is 90.63%, which is 25.18% higher than that in L-NT. The higher event reliability in L-ETX is due to the facts that the routes used in L-ETX are shorter than those in L-NT and the reliability of the links used in L-ETX is higher than that in L-NT, as shown in Figure 12 and Table III respectively. Due to the same reason, L-ETX achieves significantly higher energy efficiency than L-NT, as shown in Figures 11 and 13. For instance, the average number of packet transmissions required in delivering a packet to the base station in L-ETX is 2.82, which is 3.75 times less than that in L-NT.

From Table III, we see that the links used in L-ETX are longer yet more reliable than those in L-NT. This implies that L-ETX enables nodes to choose better routes in forwarding data and thus leads to significantly better performance in data delivery.

The facts that L-ETX uses shorter-hop-length routes and that the links used in L-ETX are longer yet more reliable than those in L-NT also suggest that, for the same requirement on end-to-end data delivery reliability, the latency and latency jitter in data delivery are smaller in L-ETX than in L-NT. Higher reliability also implies less variability and better predictability in data delivery performance (e.g., latency), because, given a link reliability p , the variability (more precisely, coefficient-of-variation) of packet transmission status (i.e., success or failure)

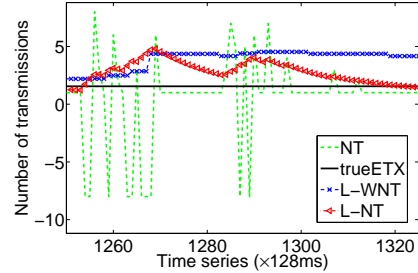


Fig. 15. Time series of estimated L-WNT and L-NT for a link of length 9.15 meters (i.e., 30 feet)

is $\sqrt{\frac{1-p}{p}}$ and it decreases as p increases. For instance, the standard deviation of the route transmission counts (and thus the delivery latency) for successfully delivered packets in L-ETX tends to be less than that in L-NT as shown in Figure 14. Therefore, compared with L-NT, L-ETX achieves a higher degree of predictability in routing performance, which is important for mission-critical networked sensing and control.

Variants of L-NT and L-ETX. Counterintuitively, Figures 10 and 11 show that L-WNT performs worse than L-NT, and Table III shows that L-WNT chooses worse routes than L-NT does. Through careful analysis, we find out that the cause for the worse performance of L-WNT is that, even though L-WNT is a more stable estimator than L-NT, it is slower (i.e., less agile) in adapting to link property changes. The slow convergence in L-WNT further exacerbates the error in NT-based estimation and leads to larger estimation error compared with L-NT, especially in the presence of dynamics. This can be seen from Figure 15 which shows the time series of the estimated ETX values in L-WNT and L-NT for a link of length 9.15 meters (i.e., 30 feet).

As expected, L-NADV performs slightly worse than L-ETX, as shown in Figure 10, Figure 11, and Table III. This is due to the larger estimation errors in L-NADV, especially in the presence of transmission failures. This can be seen from Figure 16 which presents the time series of the estimated ETX values in L-NADV and L-ETX for a link of length 9.15 meters (i.e., 30 feet).

Route stability. Table IV shows the route stability measured by comparing the routes taken by every two consecutive packets. We see that L-ETX (and its variant L-NADV) is

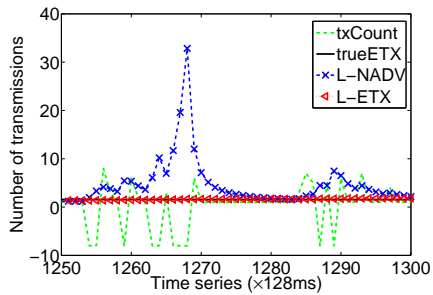


Fig. 16. Time series of estimated L-NADV and L-ETX for a link of length 9.15 meters (i.e., 30 feet)

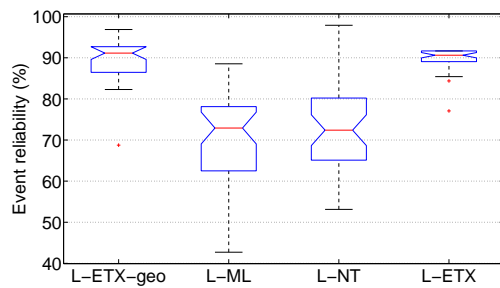


Fig. 17. Event reliability

| Two consecutive routes (%) | L-NT | L-WNT | L-ETX | L-NADV |
|----------------------------------|-------|-------|-------|--------|
| Same | 36.55 | 42 | 99.94 | 99.97 |
| Diff. routes but same hop length | 17.08 | 11.18 | 0.03 | 0.03 |
| Increased hop length | 23.96 | 24.19 | 0.03 | 0 |
| Decreased hop length | 22.41 | 22.63 | 0 | 0 |

TABLE IV

ROUTE STABILITY MEASURED BY COMPARING THE ROUTES TAKEN BY EVERY TWO CONSECUTIVE PACKETS

very stable and seldom changes route (only at a probability of $\sim 0.03\%$), yet L-NT (and its variant L-WNT) tends to be much more unstable. The fact that nodes seldom change routes in L-ETX also shows that initial link sampling is able to identify the best forwarders for most nodes in L-ETX. In mostly static networks, high stability in routing not only helps facilitate other control logics such as QoS-oriented structuring and scheduling, it also improves the predictability of routing performance, which is important for mission-critical networked sensing and control. Detailed study of these is a part of our future work.

IV. DISCUSSION

In Sections II and III, we have mainly studied the two representative data-driven protocols L-NT and L-ETX, and the study is mainly based on the regular 7×7 event traffic trace and testbed configuration. In this section, we discuss two more data-driven protocols which are related to L-ETX and/or L-NT, and we comparatively study L-ETX and L-NT with other traffic patterns and network configurations. We also compare the achievable throughput in L-ETX and L-NT respectively.

Other data-driven protocols. We implement the protocol L-ETX-geo that is a geographic-version of L-ETX and uses the ETD metric (as discussed in Section II-C); we also implement the protocol L-ML which is the same as L-NT except for the fact the MAC latency carried in MAC feedback is used to measure link quality and the routing objective is to minimize the end-to-end MAC latency in packet delivery. L-ML is very similar to L-NT since, given a certain degree of channel contention, the number of transmissions determine the MAC latency.

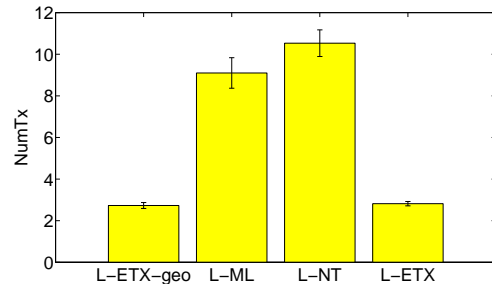


Fig. 18. Average number of transmissions per packet delivered, with the error bar representing the confidence intervals at the 95% confidence level

For the same testbed and traffic setup as in Section III-A, Figure 17 shows the event reliability, and Figure 18 shows the average number of transmissions per packet delivered in different protocols. Even though detailed study of geographic routing as compared with non-geographic, distance-vector routing is a non-trivial research issue itself and is beyond the scope of this paper, we see that L-ETX-geo achieves similar performance (e.g., statistically equal median event reliability at 95% confidence level) as L-ETX in our testbed where nodes are uniformly distributed. We also observe that L-ML performs similar to L-NT, and the event reliability and energy efficiency in L-ML are lower than those in L-ETX.

Other traffic load. Using the same event traffic trace as in Section III-A, we control the set of nodes that actually generate source packets to imitate events of different sizes. We have experimentally compared L-ETX and L-NT using two event size: 3×3 where the nodes in the farthest 3×3 subgrid from the base station generate packets, and 5×5 where the nodes in the farthest 5×5 subgrid from the base station generate packets. We observe similar phenomena for both event size configurations, and here we only present the data for the 5×5 configuration only.

For the same testbed setup as in Section III-A, Figure 19 shows the event reliability, and Figure 20 shows the average number of transmissions per packet delivered in different protocols. We see that, in the case of lighter traffic load, L-ETX still achieves higher event reliability and energy efficiency (as measured in the number of transmissions required in delivering a packet to the base station) than L-NT. Compared with the case shown in Figure 10, the event reliability of L-NT is lower

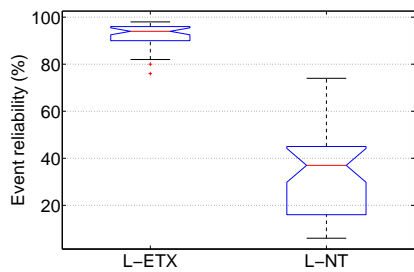


Fig. 19. 5x5: event reliability

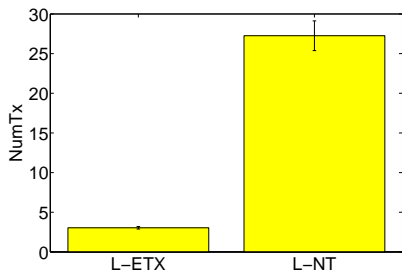


Fig. 20. 5x5: average number of transmissions per packet delivered, with the error bar representing the confidence intervals at the 95% confidence level

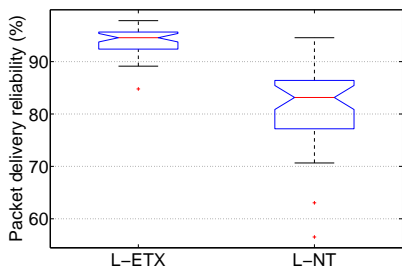


Fig. 21. Periodic traffic: packet delivery reliability

because the average distance between the traffic sources and the base station is larger in this case, which implies longer routing hops.

Periodic traffic. To understand routing performance in periodic data collection applications, we experimentally compare performance of different routing protocols in delivering periodic traffic. To this end, we let all the nodes except for the base station in a 7×7 grid periodically generate packets, where the time interval between any two consecutive packets is a random variable uniformly distributed between 10 seconds and 20 seconds. For the same testbed setup as in Section III-A, Figure 21 shows the packet delivery reliability, and Figure 22 shows the average number of transmissions per packet delivered in different protocols. We see that L-ETX outperforms L-NT in delivering periodic traffic. Compared with the case of event traffic discussed in Section III-A, the packet delivery reliability is slightly higher, because the traffic load and thus channel contention/collision is slightly lighter for the periodic traffic pattern we study here. Due to

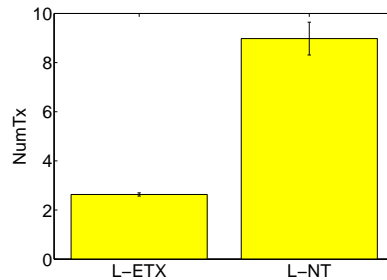


Fig. 22. Periodic traffic: average number of transmissions per packet delivered, with the error bar representing the confidence intervals at the 95% confidence level

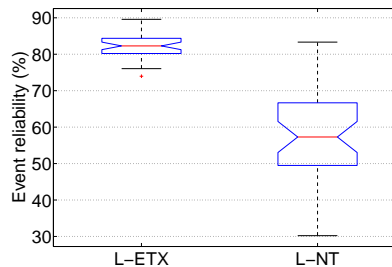


Fig. 23. Sparser network: event reliability

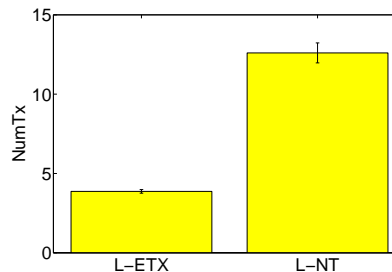


Fig. 24. Sparser network: average number of transmissions per packet delivered, with the error bar representing the confidence intervals at the 95% confidence level

similar reasons, the average number of transmissions required to deliver a packet is smaller in this periodic traffic pattern.

Sparser network. To understand whether the relative performance among different protocols is consistent across different network densities (e.g., number of neighbors for each node), we change the radio transmission power to -17dBm (i.e., power level 2). With a transmission power of -17dBm, the average number of neighbors per node is around 8 in the testbed. Then for the same node deployment and traffic trace as in Section III-A, Figure 23 shows the event reliability, and Figure 24 shows the average number of transmissions per packet delivered in different protocols. We see that L-ETX achieves higher event reliability and energy efficiency than L-NT. Compared with the case when the radio transmission power is -14dBm, the event reliability in a protocol is lower when the power level is -17dBm because the routing hop length increases as a result of the reduced power level.

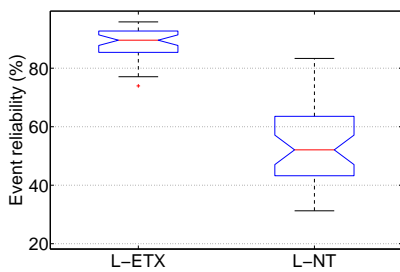


Fig. 25. Random topology: event reliability

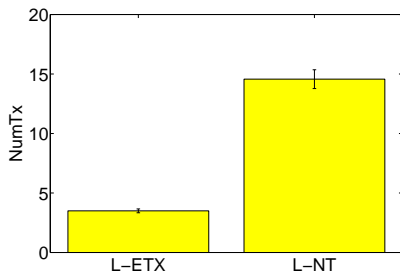


Fig. 26. Random topology: average number of transmissions per packet delivered, with the error bar representing the confidence intervals at the 95% confidence level

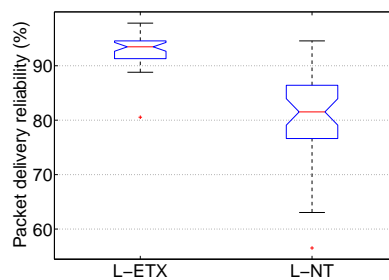


Fig. 27. Slowly moving base station: packet delivery reliability

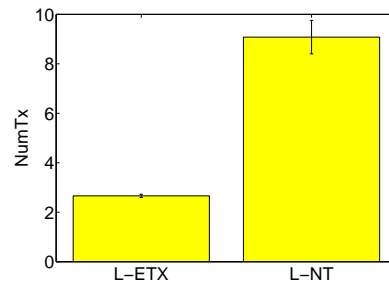


Fig. 28. Slowly moving base station: average number of transmissions per packet delivered, with the error bar representing the confidence intervals at the 95% confidence level

Random topology. Instead of deploying 49 nodes in a regular 7×7 grid, we deploy 49 nodes in a randomly selected set of 49 grid points from the 14×7 grid space as shown in Figure 2(b). Then for the same traffic trace as in Section III-A, Figure 25 shows the event reliability, and Figure 26 shows the average number of transmissions per packet delivered in different protocols. We see that L-ETX achieves significantly higher event reliability and energy efficiency than L-NT. Compared with the case when nodes are deployed in a 7×7 grid, the event reliability in a protocol is lower in the random topology because the routing hop length increases as a result of increased average spacing between nodes.

Slowly-moving base station. The focus of this paper is mainly on static sensor networks. But to get a preliminary sense of how different protocols perform in semi-static sensor networks, we study the simple scenario where the base station moves at a slow speed. This can simulate the scenario where a base station slowly moves around a field to collect sensing data. To this end, we use the same 7×7 grid of the Kansei testbed as in Section III-A, but we slowly move the base station from one corner of the grid to another corner. More specifically, the base station moves along the boundary of the grid from one corner to another corner, and the movement is such that the time taken to move from one grid point to the next neighboring grid point is uniformly distributed between 4 minutes and 5 minutes. To simulate periodic data collection, we use the “periodic traffic” pattern discussed earlier in this section; that is, each non-base-station node periodically generates packets during the experiment, where the time interval between any two consecutive packets is a

random variable uniformly distributed between 10 seconds and 20 seconds. Figure 27 shows the packet delivery reliability, and Figure 28 shows the average number of transmissions per packet delivered in different protocols. Compared with the case of “periodic traffic” with static base station (as shown in Figures 21 and 22), the performance of both L-ETX and L-NT slightly degenerates when the base station moves, for instance, $\sim 1.43\%$ decrease in average packet delivery reliability and $\sim 1.12\%$ increase in the average number of transmissions required to deliver a packet to the base station. This is because it takes time⁵ for the routing to converge, and the routing performance is slightly worse during convergence for both L-ETX and L-NT (e.g., $\sim 5\%$ decrease in average packet delivery reliability during routing convergence). Nonetheless, L-ETX still performs better than L-NT in this case of slowly moving base station. How different data-driven link estimation methods compare in general mobile networks is an important but non-trivial problem to study, since both the link estimation method and the routing protocol (e.g., that for disseminating the estimated link quality information) affect the overall routing performance. In general mobile networks, we expect that L-ETX has to be adapted to address the challenges of node mobility, and techniques proposed in [19] may be explored together with L-ETX. Detailed study of this, however, is beyond the scope of this paper, and we relegate it as a problem for future study.

Network throughput. To measure network throughput, we

⁵It takes about 1 minute for the routing to converge in our experiment setup when the base station moves from one grid point to the next neighboring grid point.

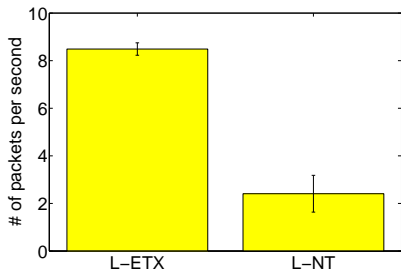


Fig. 29. Throughput

let source nodes send packets to the base station at the highest speed allowable by the system (e.g., system software and radio). We use the same testbed setup as in Section III-A, but in order not to overload the network too much, we only let nodes in the farthest 2×2 subgrid from the base station generate traffic. Figure 29 shows the number of unique packets that are delivered to the base station per second. We see that L-ETX achieves a higher throughput than L-NT. Given that the highest one-hop throughput is about 42.93 packets/second for Mica2 motes with B-MAC (the default MAC component of TinyOS) and that, in multi-hop networks, even an ideal MAC can achieve no more than $\frac{1}{4}$ of the throughput that a single-hop transmission can achieve [31], the theoretical upper limit on achievable throughput in multi-hop Mica2 networks is 10.73 packets/second. The throughput in L-ETX is 8.49 packets/second in our experiment, which is 79.12% of the upper limit.

V. RELATED WORK

Link properties in wireless sensor networks and 802.11 networks have been well studied in [3], [4], [32], [1], [2]. Experiment-based interference models have also been proposed for Mica2 radios [33] and 802.11 radios [34]. It is observed that wireless links assume complex properties, such as wide-range non-uniform packet delivery rates, loose correlation between distance and packet delivery rate, link asymmetry, and temporal variations. The β -factor [22] was proposed to identify the burstiness of wireless links and then to help schedule packet transmissions for taking advantage of bursts of successful transmissions while avoiding bursts of transmission failures at the same time. Orthogonal to these studies, our work here comparatively study the behaviors of different data-driven methods of estimating wireless link properties for routing, with a special focus on the ETX metric.

Differences between broadcast and unicast and their impact on the performance of AODV were first discussed in [7] and [8], and the authors discussed reliability-based mechanisms (e.g., those based on RSSI or SNR) for blacklisting bad links. The authors also proposed mechanisms, such as enforcing SNR threshold on control packets, to ameliorate the negative impact of the differences, and the authors of [7] studied the impact of packet size, packet rate, and link reliability threshold on the end-to-end delivery rate in AODV. Nonetheless, the proposed solutions were still based on beacon exchanges among neighbors.

Zhang *et al.* systematically studied the inherent drawbacks of beacon-based link estimation and proposed to use unicast MAC feedback as the basis of link estimation in IEEE 802.11b and mote networks [10], [20]. Methods of using both MAC feedback and beacon packets in link estimation were also proposed in MintRoute [6], EAR [13], and four-bit-estimation [11]; SPEED [12], NADV [15], and CARP [14] also used MAC feedback in link estimation and route selection. Nonetheless, there has been no systematic study on the impact that the different ways of using MAC feedback have on routing behaviors, and our study in this paper fills this vacuum and provides insight into the principles of using MAC feedback in data-driven link estimation and routing.

Other routing metrics and protocols [35], [36], [37], [38], [39], [40], [41] have also been proposed for various optimization objectives (e.g., energy efficiency). The findings of this paper can be applied to these schemes to help improve the accuracy of estimating link and path properties. Directed diffusion [42] provides a framework for routing in sensor networks, and the findings of this paper can also be applied to this framework to help select high-performance routes in data forwarding. The CTP protocol [18] was recently proposed to address issues such as detecting routing loops and maintaining routing correctness/consistency at low cost. The study of CTP protocol is orthogonal to our focus on the behaviors of different data-driven link estimation methods in this paper.

Rather than selecting the next-hop forwarder before data transmission, opportunistic routing protocols that take advantage of spatial diversity in wireless transmission have been proposed [43], [44], [45], [46]. In these protocols, the forwarder is selected, through coordination among receivers, in a reactive manner after data transmission. Link estimation can still be helpful in these protocols since it can help effectively select the best set of listeners [43]. Therefore, findings of this paper can be useful in opportunistic routing too.

Draves *et al.* comparatively studied several routing metrics in the context of beacon-based link estimation and routing [47], and they have found out that ETX is an effective metric for routing in mostly static wireless networks. Broch *et al.* have also comparatively studied the behaviors of mobile ac-hoc network routing protocols DSDV, TORA, DSR, and AODV [48]. Our work in this paper focuses on the different methods of using unicast MAC feedback to estimate the metric ETX in mostly static networks, and we have demonstrated the importance of choosing the right method among seemingly similar approaches.

VI. CONCLUDING REMARKS

Through mathematical analysis and measurement based study, we have examined the impacts that different data-driven link estimation methods have on routing behaviors. We have shown that the variability of parameters being estimated significantly affects the reliability, latency, energy efficiency, and predictability of data-driven link estimation and routing, and it should be an important criterion to consider when choosing the data-driven link estimation method. We have shown that L-ETX is a precise, stable method of estimating

the ETX of data transmissions, and that a seemingly similar method L-NT of estimating ETX and approaches based on MAC latency perform much worse in terms of packet delivery reliability, energy efficiency, and routing stability. These findings elucidate the subtleties of data-driven link estimation and provide guidelines on how to effectively use MAC feedback in link estimation.

The experimental analysis of this paper is based on networks of CC1000 radios. Even though we expect the findings of this paper to be valid for networks of IEEE 802.15.4 radios, systematic evaluation of this conjecture is a part of our future work. We have focused on accurate estimation of the ETX routing metric in this paper, identifying accurate estimation methods for other routing metrics such as mETX [37] and CTT [41] is also an important task to pursue for supporting different optimization objectives in routing.

ACKNOWLEDGMENT

We thank Elif Uysal-Biyikoglu and George Yin for discussions on link estimation.

REFERENCES

- [1] D. Aguayo, J. Bicket, S. Biswas, G. Judd, and R. Morris, "Link-level measurements from an 802.11b mesh network," in *ACM SIGCOMM*, 2004.
- [2] D. Kotz, C. Newport, and C. Elliott, "The mistaken axioms of wireless-network research," Dartmouth College, Computer Science, Tech. Rep. TR2003-467, July 2003.
- [3] J. Zhao and R. Govindan, "Understanding packet delivery performance in dense wireless sensor networks," in *ACM SenSys*, 2003.
- [4] M. Zuniga and B. Krishnamachari, "An analysis of unreliability and asymmetry in low-power wireless links," *ACM Transactions on Sensor Networks*, vol. 3, no. 2, 2007.
- [5] D. S. J. D. Couto, D. Aguayo, J. Bicket, and R. Morris, "A high-throughput path metric for multi-hop wireless routing," in *ACM MobiCom*, 2003.
- [6] A. Woo, T. Tong, and D. Culler, "Taming the underlying challenges of reliable multihop routing in sensor networks," in *ACM SenSys*, 2003.
- [7] I. Chakeres and E. Belding-Royer, "The utility of hello messages for determining link connectivity," in *WPMC*, 2002.
- [8] H. Lundgren, E. Nordstrom, and C. Tschudin, "Coping with communication gray zones in IEEE 802.11b based ad hoc networks," in *ACM WoWMoM*, 2002.
- [9] A. Willig, "A new class of packet- and bit-level models for wireless channels," in *IEEE PIMRC*, 2002.
- [10] H. Zhang, A. Arora, and P. Sinha, "Link estimation and routing in sensor network backbones: Beacon-based or data-driven?" *IEEE Transactions on Mobile Computing*, May 2009.
- [11] R. Fonseca, O. Gnawali, K. Jamieson, and P. Levis, "Four-bit wireless link estimation," in *ACM HotNets*, 2007.
- [12] T. He, B. Stankovic, C. Lu, and T. Abdelzaher, "SPEED: A stateless protocol for real-time communication in sensor networks," in *IEEE ICDCS*, 2003.
- [13] K.-H. Kim and K. G. Shin, "On accurate measurement of link quality in multi-hop wireless mesh networks," in *ACM MobiCom*, 2006.
- [14] R. Krishnan, A. Raniwala, and T. Cker Chiueh, "Design of a channel characteristics-aware routing protocol," in *IEEE INFOCOM miniconference*, 2008.
- [15] S. Lee, B. Bhattacharjee, and S. Banerjee, "Efficient geographic routing in multihop wireless networks," in *ACM MobiHoc*, 2005.
- [16] H. Zhang, A. Arora, and P. Sinha, "Learn on the fly: Data-driven link estimation and routing in sensor network backbones," in *25th IEEE International Conference on Computer Communications (INFOCOM)*, 2006.
- [17] "Exscal project," <http://www.cse.ohio-state.edu/exscal>, 2004.
- [18] O. Gnawali, R. Fonseca, K. Jamieson, D. Moss, and P. Levis, "Collection tree protocol," in *ACM SenSys*, 2009.
- [19] M. Kim and B. Noble, "Mobile network estimation," in *ACM MobiCom*, 2001.
- [20] H. Zhang, L. Sang, and A. Arora, "Experimental analysis of link estimation methods in low power wireless networks," Tech. Rep.
- [21] A. Keshavarzian, E. Uysal-Biyikoglu, D. Lal, and K. Chintalapudi, "From experience with indoor wireless networks: A link quality metric that captures channel memory," *IEEE Communications Letters*, VOL. 11, NO. 9, SEPTEMBER 2007, vol. 11, no. 9, 2007.
- [22] K. Srinivasan, M. A. Kazandjieva, S. Agarwal, and P. Levis, "The β -factor: Measuring wireless link burstiness," in *ACM SenSys*, 2008.
- [23] E. Ertin, A. Arora, R. Ramnath, M. Nesterenko, V. Naik, S. Bapat, V. Kulathumani, M. Sridharan, H. Zhang, and H. Cao, "Kansei: A testbed for sensing at scale," in *IEEE/ACM IPSN/SPOTS*, 2006.
- [24] P. Dutta, M. Grimmer, A. Arora, S. Bibyk, and D. Culler, "Design of a wireless sensor network platform for detecting rare, random, and ephemeral events," in *IEEE/ACM IPSN/SPOTS*, 2005.
- [25] "Crossbow Mica2 motes," http://www.xbow.com/Products/Product_pdf_files/Wireless_pdf/MICA2_Datasheet.pdf.
- [26] "Chipcon CC1000 RF transceiver," <http://focus.ti.com/lit/ds/symlink/cc1000.pdf>.
- [27] "TinyOS," <http://www.tinyos.net/>.
- [28] J. Polastre, J. Hill, and D. Culler, "Versatile low power media access for wireless sensor networks," in *ACM SenSys*, 2004.
- [29] P. C. Ng and S. C. Liew, "Throughput analysis of IEEE 802.11 multi-hop ad hoc networks," *IEEE/ACM Transactions on Networking*, vol. 15, no. 2, 2007.
- [30] "An event traffic trace for sensor networks," <http://www.cs.wayne.edu/~hzhang/group/publications/Lites-trace.txt>.
- [31] J. Li, C. Blake, D. S. D. Couto, H. I. Lee, and R. Morris, "Capacity of ad hoc wireless networks," in *ACM MobiCom*, 2001.
- [32] K. Srinivasan, P. Dutta, A. Tavakoli, and P. Levis, "Understanding the causes of packet delivery success and failure in dense wireless sensor networks," Stanford University, Tech. Rep. SING-06-00, 2006.
- [33] D. Son, B. Krishnamachari, and J. Heidemann, "Experimental analysis of concurrent packet transmissions in low-power wireless networks," in *ACM SenSys*, 2006.
- [34] L. Qiu, Y. Zhang, F. Wang, M. K. Han, and R. Mahajan, "A general model of wireless interference," in *ACM MobiCom*, 2007.
- [35] Q. Cao, T. He, L. Fang, T. Abdelzaher, J. Stankovic, and S. Son, "Efficiency centric communication model for wireless sensor networks," in *IEEE INFOCOM*, 2006.
- [36] Y. Gu and T. He, "Data forwarding in extremely low duty-cycle sensor networks with unreliable communication links," in *ACM SenSys*, 2007.
- [37] C. E. Koksal and H. Balakrishnan, "Quality-aware routing metrics for time-varying wireless mesh networks," *IEEE JSAC*, vol. 24, no. 11, 2006.
- [38] J. C. Park and S. K. Kasera, "Expected data rate: An accurate high-throughput path metric for multi-hop wireless routing," in *IEEE SECON*, 2005.
- [39] D. Pompili, T. Melodia, and I. F. Akyildiz, "Routing algorithms for delay-insensitive and delay-sensitive applications in underwater sensor networks," in *ACM MobiCom*, 2006.
- [40] M. Wachs, J. I. Choi, J. W. Lee, K. Srinivasan, Z. Chen, M. Jain, and P. Levis, "Visibility: A new metric for protocol design," in *ACM SenSys*, 2007.
- [41] H. Zhai and Y. Fang, "Impact of routing metrics on path capacity in multirate and multihop wireless ad hoc networks," in *IEEE ICNP*, 2006.
- [42] C. Intanagonwivat, R. Govindan, and D. Estrin, "Directed diffusion: A scalable and robust communication paradigm for sensor networks," in *ACM MobiCom*, 2000.
- [43] S. Biswas and R. Morris, "ExOR: Opportunistic multi-hop routing for wireless networks," in *ACM SIGCOMM*, 2005.
- [44] S. Chachulski, M. Jennings, S. Katti, and D. Katabi, "Trading structure for randomness in wireless opportunistic routing," in *ACM SIGCOMM*, 2007.
- [45] T. He, B. M. Blum, Q. Cao, J. A. Stankovic, S. H. Son, and T. F. Abdelzaher, "Robust and timely communication over highly dynamic sensor networks," *Real-Time Systems Journal*, vol. 37, 2007.
- [46] F. Ye, G. Zhong, S. Lu, and L. Zhang, "GRAdient Broadcast: A robust data delivery protocol for large scale sensor networks," in *IEEE IPSN*, 2003.
- [47] R. Draves, J. Padhye, and B. Zill, "Comparison of routing metrics for static multi-hop wireless networks," in *ACM SIGCOMM*, 2004.
- [48] J. Broch, D. A. Maltz, D. B. Johnson, Y.-C. Hu, and J. Jetcheva, "A performance comparison of multi-hop wireless ad hoc network routing protocols," in *ACM MobiCom*, 1998.